LIDAR STRIP ADJUSTMENT USING AUTOMATICALLY RECONSTRUCTED ROOF SHAPES

M. Rentsch *, P. Krzystek

University of Applied Sciences Muenchen, Department of Geographic Information Sciences, 80333 Munich, Germany
- (rentsch, krzystek)@hm.edu

Commission I, WG I/2

KEY WORDS: LIDAR, Reconstruction, Adjustment, Building, Point Cloud, Quality

ABSTRACT:

LiDAR systems have been established as technology for fast and high-resolution acquisition of 3D point clouds. In general, LiDAR data acquisition is conducted by private companies who are also responsible for processing and quality control. However, in many cases a subsequent quality assessment of overlapping LiDAR strips still reveals apparent horizontal and vertical offsets which are caused by undetected systematic errors (e.g. insufficient calibration and strip adjustment). The presented work covers methods for the detection of remaining discrepancies in overlapping LiDAR strips with main focus on the development of a new precise 3D measurement technique based on intersecting roof ridge lines and roof planes which are automatically reconstructed from the LiDAR point clouds in overlapping strips. The coordinate differences between conjugate intersection points are incorporated in an adjustment process to resolve for the residual errors of each LiDAR strip separately. The new 3D reconstruction method can also take advantage of full waveform measurements like pulse width and intensity which are decomposed from the waveforms. Finally, the LiDAR strips are corrected and validated by checking the correspondence among neighbouring strips. The quality control system has been successfully applied to pre-processed and adjusted LiDAR strips. In general, the results show that significant discrepancies mainly in position still exist. After the adjustment of 8 strips (altitude 1000 m) using precise 3D measurements, the relative horizontal displacements between adjacent strips are improved by more than 70 %.

1. INTRODUCTION

Geospatial databases are essential for describing the Earth's surface with the requirement of high quality and being up-to-date. LiDAR, also known as airborne laser scanning (ALS), has been established as technology for fast and high-resolution acquisition of the terrain surface. Major secondary products of LiDAR data are DTMs and DSMs for various applications in geoscience. Due to the rapidly growing amount of LiDAR data in the recent years, the users were increasingly faced with the cost-intensive collection, continuation and quality assessment of geospatial databases. The dominant sources affecting the quality of LiDAR derived products are residual errors coming from insufficient calibration and strip adjustment, and errors in data classification and filtering. In most cases, LiDAR data acquisition is conducted by private companies who also perform the pre-processing, the classification and the quality control. Nevertheless, subsequent quality investigations still exhibit horizontal and vertical offsets which are clearly visible at distinct objects (e.g. roof profiles) in overlapping areas of adjacent tracks (Figure 5).

In the literature, various methods have been proposed for the adequate measurement of horizontal and vertical offsets. Due to the fact that the direct comparison of LiDAR points from different strips is not feasible, selected features which could be reconstructed from the laser point clouds are considered.

Kilian et al. (1996) are using ground planes of buildings for measuring building corners and the corresponding corner coordinates from the laser data. Two methods for detecting offset values are based on a TIN structure deduced from the laser points. Burman (2002) derives the height discrepancy for a laser point of the first strip by relating the position to the TIN surface of the second strip. Maas (2002) is generating local TINs for small areas in overlapping strips and derives 3D offsets through a least squares matching between the selected subsets. For both approaches the laser reflectance (intensity) discrepancies were also included serving as a helpful tool in regions with low height variations but good intensity contrast. The focus in Filin (2003), Filin and Vosselman (2004), Pfeifer et al. (2005) and Friess (2006) is on the extraction of suitable planar segments (natural or man-made) for the determination of corresponding tie and control elements in different LiDAR strips. Filin (2003) emphasizes that the error recovery can benefit from object surfaces with different slopes. Pfeifer et al. (2005) recommend several selection criteria, leading to at least 20 corresponding segments per overlay. Finally, the offsets are determined by comparing the barycenters of the selected surfaces. However, the localization of the barycenters depends on the laser point coverage representing the tie surfaces.

In the recent years, the emphasis was also on the extraction of building roof shapes as tie elements. The fully 3D adjustment approach of Kager (2004) incorporates artificially tie points resulting from intersection of at least three planar roof elements. Pothou et al. (2008) conduct the estimation of boresight misalignment parameters by comparing LiDAR derived roof surfaces with photogrammetrically reconstructed reference surfaces. An extension with respect to these approaches is the

---

* Corresponding author.

addition of extracted roof ridge lines from roof plane intersections. Ahokas et al. (2004) are using ridge lines for a comparison study with repeated ALS observations. Schenk et al. (1999) present a quality accuracy study for LiDAR data in an urban area by comparing reconstructed roof ridge lines after laser point segmentation with photogrammetric DEM measurements and directly measured roof ridge points. Habib et al. (2008) are computing corresponding linear features from intersections of roof planes in overlapping LiDAR strips. The linear features are represented by its end points and their coordinate discrepancies between different strips serve as input for a strip adjustment and quality control. Vosselman (2008) presents a largely automatic procedure for assessing the planimetric accuracy of three LiDAR surveys in the Netherlands. Relative horizontal shifts between overlapping areas of adjacent strips are measured by detection and comparison of reconstructed roof ridge lines from the laser data. In this approach, the center points of corresponding ridge lines are derived. However, if the laser point clouds of different strips are not describing the same roof outline, the lengths of reconstructed roof ridge lines might differ resulting in misleading positions of the line centers.

The main focus of the presented work is on the development of a new method for the precise 3D measurement of remaining horizontal and vertical offsets between overlapping areas of adjacent LiDAR strips. For this purpose, appropriate roof shapes with crossing ridge lines are reconstructed from the laser point clouds. Then, 2D and 3D points are derived by intersecting the roof planes and ridge lines for each strip separately. The approach is basically suitable for full waveform data comprising the pulse energy (viz. the intensity) and the pulse width as additional laser point attributes. The strip-to-strip coordinate differences of the 2D and 3D intersection points represent the displacements which are mainly caused by residual systematic errors concerning the laser range measurement, GPS position, IMU attitudes and the alignment of the LiDAR system components. The relation of measured horizontal and vertical offsets and residual errors is modeled by a simplified 3D transformation. By introducing the offset measurements as observations, the residual errors for shifts and rotations are resolved by means of an adjustment approach and finally, the resulting corrections are applied to the laser points.

The paper is organized as follows. Section 2 highlights the strip adjustment model and the reconstruction of roof shapes. Section 4 addresses the results we obtained with a dataset comprising 8 overlapping strips. Finally, the results are discussed in Section 5 with conclusions given in Section 6.

2. METHODS

2.1 Concept

LiDAR surveys are usually conducted by scanning the terrain surface in a strip-wise manner with an appropriate across-track overlap. There are three types of error sources affecting the acquired laser point coordinates: Unsystematic gross errors (blunders), systematic errors and random errors (noise). Whereas gross errors are mostly discarded within the pre-processing of laser measurements, random errors coming from instrument noise will always remain (Friess, 2006). Thus, for a mathematical formulation, the measured discrepancies between overlapping areas of adjacent strips are exclusively related to

systematic residual errors caused by insufficient calibration of the LiDAR system components or inadequate strip adjustment.
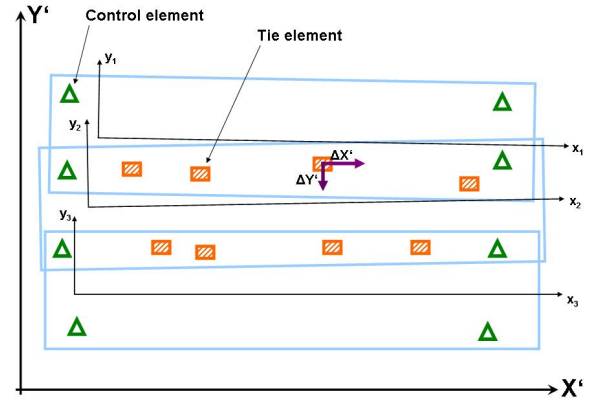

Figure 1. Sample configuration of LiDAR strips with control (green) and tie elements (orange). As example, relative horizontal offsets ΔX' and ΔY' between overlapping strips are measured for a tie element (violet)

Comprehensive mathematical formulations for the relationship between observed laser point coordinates and system-dependent parameters are given by various authors (Kilian et al. 1996; Burman, 2002; Schenk, 2001; Filin, 2003). Due to the strip-wise acquisition of LiDAR surveys, the systematic errors are supposed to affect the coordinate offsets for each strip separately (Figure 1). For simplification, some assumptions are defined for the mathematical model of our approach (Equation 1). First, time dependent portions are not considered. The rotation angles (roll and heading) are assumed as small values and no rotation angle along the y-axis of a strip i is applied. This means that we do not compensate for a pitch angle error which causes essentially a horizontal shift in the laser points. The error model resp. the observation equations are established in a local strip coordinate system in which the strip centroids represent the origin and the local x-axis is approximately aligned to the flight direction (Vosselman and Maas, 2001).

$$\begin{pmatrix} X'_{ik} \\ Y'_{ik} \\ Z'_{ik} \end{pmatrix} = \begin{pmatrix} 1 & -\Delta h_i & 0 \\ \Delta h_i & 1 & -\Delta r_i \\ 0 & \Delta r_i & 1 \end{pmatrix} \cdot \begin{pmatrix} x_{ik} - x_i^s \\ y_{ik} - y_i^s \\ z_{ik} - z_i^s \end{pmatrix} + \begin{pmatrix} X_{0i} \\ Y_{0i} \\ Z_{0i} \end{pmatrix} \qquad (1)$$

where

$X'_{ik}, Y'_{ik}, Z'_{ik}$	Coordinates of laser point k of corrected strip i
$\Delta r_i, \Delta h_i$	Rotation angles for roll and heading of strip i
x_{ik}, y_{ik}, z_{ik}	Coord. of laser point k of uncorrected strip i
X_{0i}, Y_{0i}, Z_{0i}	Shifts of uncorrected strip i
x_i^s, y_i^s, z_i^s	Centroid of uncorrected strip i

The unknown parameters of each strip i are found in a combined adjustment using control and tie elements. Control and tie elements are usually horizontal, vertical or 3D elements measured by an appropriate measurement technique.

2.2 3D Measurement Technique 'Roof Shapes'

There are three implemented methods to derive spatial offsets between overlapping laser strips, for more details see Rentsch and Krzystek (2009). Main interest is given here on the precise measurements of 3D offsets between neighbouring laser strips.

2.2.1 3D Measurement Technique 'Roof Shapes': The new method has been developed to derive 2D as well as 3D points from the intersection of modeled roof ridge lines coming from different LiDAR strips. The main processing steps can be divided as follows: (1) Selection of buildings with appropriate roof surfaces, e.g. L-shaped or T-shaped. (2) Separation of roof points from bare Earth points. Herein, the separation is supported by predetermined building outlines or, if not available, by dividing the points according to their pre-classified point class and height values. (3) Computation of geometric and physical laser point features. At each laser point location, a local fitting RANSAC plane is computed from the surrounding points (Figure 2). According to the given point density, an appropriate search radius is determined to ensure that a predefined number of points (e.g. 30) is included. Laser points for which the height variations with respect to the local plane exceed a defined threshold (this appears for example for points on a roof ridge) are rejected. Afterwards, for each selected laser point, a list of features is determined: The xyz-components of the plane normal vector n_x, n_y and n_z, the orientation of the roof plane $po=arctan(n_x/n_y)$, the laser intensity and the pulse width. Note that the features intensity and pulse width are optional and are dedicated to full waveform LiDAR systems. They can be calculated via waveform decomposition (Reitberger et al., 2008). (4) Segmentation of roof planes by means of clustering using the derived features. A preliminary clustering of laser points is performed by means of the k-means algorithm and a given number of clusters. For each of the found clusters, common features as described before are derived and assigned. Tiny clusters with a very small number of points (e.g. 5) are apparently discarded. Then, the clusters undergo a hierarchical clustering which leads to a merging of clusters with nearly coinciding features and resulting to clearly separated roof planes. (5) Finally, an adjusting plane is computed including all laser points from each merged cluster. Laser points on small features like chimneys or dormers are detected by means of their distance to the adjusting plane and are filtered out. (6) Evaluation of roof ridge lines by means of plane intersections. The appropriate roof planes which are used for plane intersection are selected according to their features (e.g. opposite orientation) and are intersected, leading to a pair of ridge lines in the normal case. (7) Derivation of 2D points from line intersections and 3D points from plane-line intersection. Because the extracted ridge lines are representing skewed straight lines in space, a 3D intersection between them could not be carried out. However, a 2D intersection is always feasible meaning that the X- and Y-coordinates of a ridge line intersection are always ascertained. Fully 3D coordinates can be achieved by intersecting the lower of the two ridge lines with the opposite roof planes, resulting in two intersection points (Figure 3). (8) Finally, the coordinate differences of conjugate intersection points in overlapping strip areas can be calculated, revealing the spatial offsets caused by remaining shifts and rotations (Figure 4).
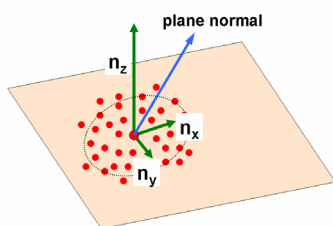
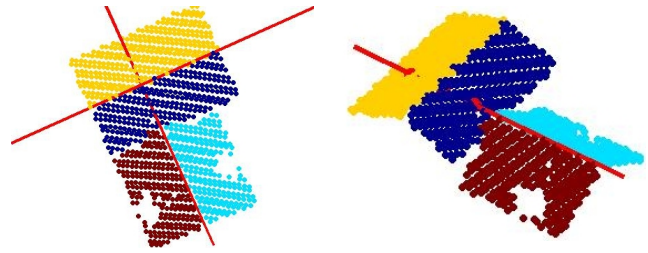Figure 2. Construction of local fitting RANSAC plane at each laser point location

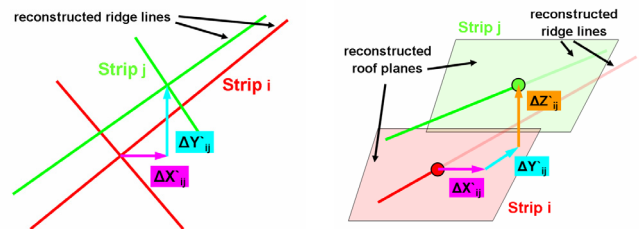Figure 3. Calculation of 2D and 3D intersection points

Figure 4. Determination of 2D and 3D offsets

2.2.2 Sensitivity Analysis: The internal precision of the measured offsets is determined by means of repeating the entire measurement process (steps 4-8) for a predefined number of runs (e.g. 20). The standard deviations are caused by variations coming from the random selection of laser points in the RANSAC-based plane adjustment (step 5). Thus, a statistical analysis is performed leading to a mean value (the offset measurement) and its standard deviation. In addition, within this analysis, outliers are detected and removed according to a 2-sigma criterion.

2.2.3 Quality Control: In many cases, the quality control in the framework of LiDAR surveys is limited to a visual inspection of adjacent laser strips in overlapping areas, e.g. by overlaying the laser point profiles of roofs or other appropriate objects. In addition, the quality assessment relies on a high extent on the personal point of view of the operator. With the proposed 3D measurement technique, the detected horizontal and vertical offsets now can be used for a numeric based quality control and are supporting the results from the visual control (Figure 5). Moreover, the results are achieved by well-defined algorithms, transparent and the basis for further processes.
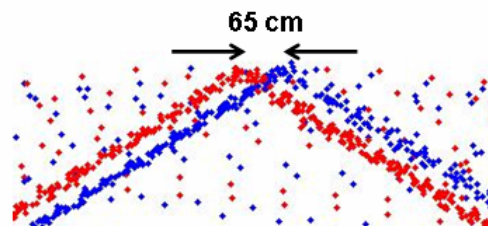
Figure 5. Large planimetric discrepancies measured at a roof showing insufficient strip adjustment.

2.3 Strip Adjustment

For this purpose, two basic types of observation equations are established. Equation (2) stands for an absolute measurement for a control element, equation (3) for a relative measurement between overlapping strips and are given as follows

$$\begin{pmatrix} X'_{ik} \\ Y'_{ik} \\ Z'_{ik} \end{pmatrix} + \begin{pmatrix} v_X \\ v_Y \\ v_Z \end{pmatrix} = \begin{pmatrix} 1 & -\Delta h_i & 0 \\ \Delta h_i & 1 & -\Delta r_i \\ 0 & \Delta r_i & 1 \end{pmatrix} \cdot \begin{pmatrix} x_{ik} - x_i^s \\ y_{ik} - y_i^s \\ z_{ik} - z_i^s \end{pmatrix} + \begin{pmatrix} X_{0i} \\ Y_{0i} \\ Z_{0i} \end{pmatrix} \quad (2)$$

$$\begin{pmatrix} \Delta X'_{ijk} \\ \Delta Y'_{ijk} \\ \Delta Z'_{ijk} \end{pmatrix} + \begin{pmatrix} v_{\Delta X} \\ v_{\Delta Y} \\ v_{\Delta Z} \end{pmatrix} = \begin{pmatrix} 1 & -\Delta h_i & 0 \\ \Delta h_i & 1 & -\Delta r_i \\ 0 & \Delta r_i & 1 \end{pmatrix} \cdot \begin{pmatrix} x_{ik} - x_i^s \\ y_{ik} - y_i^s \\ z_{ik} - z_i^s \end{pmatrix} - $$
$$\begin{pmatrix} 1 & -\Delta h_j & 0 \\ \Delta h_j & 1 & -\Delta r_j \\ 0 & \Delta r_j & 1 \end{pmatrix} \cdot \begin{pmatrix} x_{jk} - x_j^s \\ y_{jk} - y_j^s \\ z_{jk} - z_j^s \end{pmatrix} + \begin{pmatrix} X_{0i} - X_{0j} \\ Y_{0i} - Y_{0j} \\ Z_{0i} - Z_{0j} \end{pmatrix} \quad (3)$$

where X'_{ik}, Y'_{ik}, Z'_{ik} represent the measurements on a control element k in the strip i, and $\Delta X'_{ijk}$, $\Delta Y'_{ijk}$, $\Delta Z'_{ijk}$ are the offset measurements between strip i and j on a tie element k. The terms v_X, v_Y, v_Z stand for the residuals of the measurements on a control element, and $v_{\Delta X}$, $v_{\Delta Y}$, $v_{\Delta Z}$ for the residuals of the measurements on a tie element. The unknown shifts of strip i are given by X_{0i}, Y_{0i}, Z_{0i}, and the unknown rotation angles (compensating IMU rotations **roll** and **heading**) for the strip i by Δr_i and Δh_i. The coordinates x_i^S, y_i^S, z_i^S of the strip centroids are calculated from laser points of the uncorrected strip.

For the strip adjustment, 6 different observation types are introduced; type 1-3 belonging to observation equation (2), type 4-6 to equation (3). For the stochastic model, each of the observation types can be assigned with individual a-priori standard deviations reflecting their varying accuracy levels.

Obs. Type	Description
1	Absolute vertical measurement with respect to a height control element (e.g. soccer field)
2	Absolute horizontal measurements with respect to a control element
3	Absolute 3D measurements with respect to a control element
4	Relative vertical offset measurement between adjacent strips for a tie element
5	Relative horizontal offset measurement between adjacent strips for a tie element
6	Relative 3D offset measurement between adjacent strips for a tie element

Table 1. Observation types used within the strip adjustment

3. MATERIAL

The algorithms are evaluated for 8 sample adjacent LiDAR strips within a project area 'Kempten' located in Southern Bavaria and surveyed in May 2006 (Figure 6). For more than a decade, the Bavarian Office for Surveying and Geographic Information (LVG) systematically produces and delivers high-resolution DTMs with down to 1-m spacing based on airborne laser scanning. The flight surveys are conducted by several companies who are also responsible for pre-processing, georeferencing of the laser points, adjustment of the laser strips and an automatic classification of the raw laser data. Moreover, an internal quality control is performed by these contractors. Laser point clouds for first and last pulse then are delivered to the LVG. The datasets itself contain the UTM coordinates, the ellipsoidal height above GRS80, the point class derived by the flight company and the laser intensity. However, information on GPS positions and IMU attitudes are usually not available.
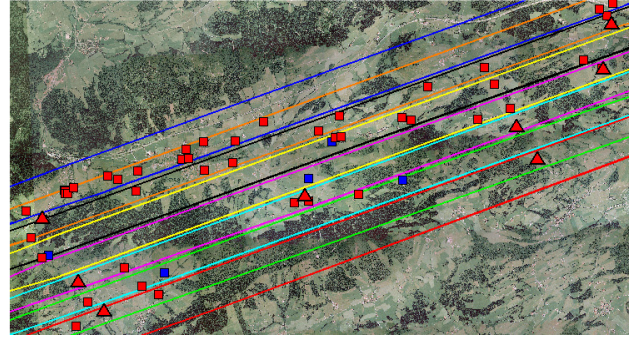

Figure 6. Test site 'Kempten'

The entire project area was flown in a strip wise manner, mostly in east-west direction except two sections containing the sample strips, which are deviated about 30 degrees against east-west. With a predefined flight altitude of 1000 m and a scan angle of 22 degrees, this led to strip width of around 800 m. 45 % were chosen as across-track overlap resulting in approximately 300 m wide common areas of neighbouring strips. The mean point density is about 1-2 points/m^2.

For the generation of 2D and 3D control points, several roof ridge lines were determined photogrammetrically by measuring sample roof ridge points in digitized aerial images with nearly the same acquisition date as the LiDAR data. Based on the image scale of 1:12400 and the pixel size of 14 μm, the measurement accuracy in the stereo model can be theoretically estimated to 17.5 cm for the planimetric and 35 cm for the height coordinates. 2D points are derived be intersecting the reconstructed ridge lines in the horizontal projection. Virtual 3D points are constructed by taking the 2D point coordinates and deriving the Z-coordinate by means of intersecting the orthogonal plane through the 2D point with the lower ridge line.

4. EXPERIMENTS

4.1 Adjustment Results

As mentioned before, the mathematical model is designed to resolve for 3 shifts and the 2 rotations compensation the IMU rotations for roll and heading for each individual strip. Optionally, the model is also capable to determine the 3 shifts and 2 rotations separately. Thus, for a pair of adjacent strips, 10 unknowns have to be resolved and 5 unknowns more for each additional strip. Figure 6 also displays the locations off all tie and control elements. The blue squares are representing tie elements with vertical offset measurements, the red ones the locations with 2D and 3D offset measurements. The red triangles stand for 2D and 3D control elements which are necessary for the absolute alignment of the LiDAR strips.

The adjustment process was performed according to the mathematical model given by equations (2) and (3) using 370 observations to resolve for the overall 24 unknown shifts and 16 unknown rotations. As mentioned before, the different observation types had to be handled individually concerning their internal precision and as a consequence, the a-priori standard deviations which were incorporated into the stochastic model. The internal standard deviations of the sensitivity analysis for the offsets using the 3D measurement technique 'roof shapes' were mostly below a 3 cm level (Figure 7).
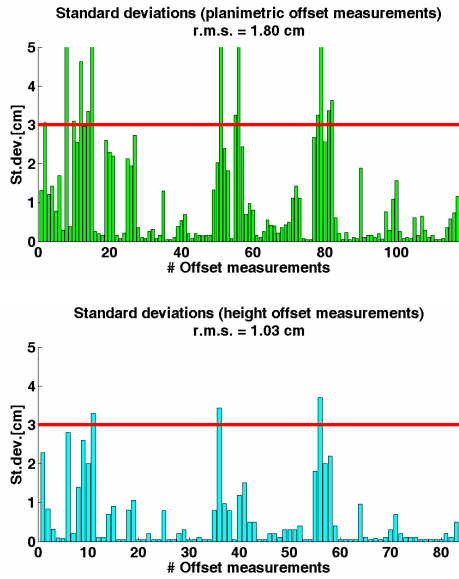
Figure 7. Internal standard deviations of planimetric (green) and height (cyan) offsets using the 3D measurement technique 'roof shapes'. The red line denotes the 3 cm level

However, several tests have shown that the assumption using these internal standard deviations as a-priori input were too optimistic. Therefore, more appropriate values were defined for the a-priori standard deviations for each observation type leading to more reasonable results (Table 2). The standard deviations after the strip adjustment for the individual observation types reflect the particular accuracy level and thus the appropriate stochastical model.

Obs. Type	sigma naught (a-posteriori) [cm]	#Obs.
1	9.4	2
2	12.7	4
3	18.6 (planimetry), 11.7 (height)	42
4	8.4	5
5	7.2	68
6	8.3 (planimetry), 6.6 (height)	249

Table 2. Standard deviations after strip adjustment for each observation type separately

The resolved unknowns for the 8 adjacent strips of the test site are listed in Table 3.

Strip	X_0 [cm]	Y_0 [cm]	Z_0 [cm]	Δr [deg]	Δh [deg]
160	77.7	29.8	17.6	0.002	-0.002
161	43.9	40.5	13.6	0.004	-0.002
162	36.6	-7.6	2.4	-0.002	-0.001
163	10.2	7.9	1.0	-0.001	-0.002
164	6.6	-16.1	1.7	0.000	-0.006
166	-26.5	3.2	7.1	0.001	-0.005
167	-36.5	-62.4	-4.8	0.001	-0.005
168	-72.0	-41.4	0.9	0.000	-0.005

Table 3. Resolved shifts and rotation angles

4.2 Strip correction and validation

The corrections were applied for each LiDAR strip using the flight trajectories which were also provided by LVG. For each laser point location, the measurement constellation was reconstructed by calculating the orthogonal plane of the trajectory including the uncorrected laser point. Then, the derived shifts and rotations resulting from the adjustment were applied to the points of each LiDAR strip separately. Finally, the 3D measurement technique was carried out for the corrected laser points revealing that the relative displacements between adjacent strips could be reduced significantly (Table 4).

	r.m.s. planimetry [cm]	r.m.s. height [cm]
before strip adjustment	35.6	9.5
after strip adjustment	10.2	6.6

Table 4. Relative displacements of 50 virtual control elements before and after strip adjustment.

5. DISCUSSION

The main focus of the present work is on a new and precise 3D measurement technique for the determination of horizontal and vertical offsets between overlapping regions of adjacent LiDAR strips. The discrepancies can be measured using the intersection points of reconstructed roof ridge lines and roof planes. Table 2 shows that the estimated accuracy of the method after the strip adjustment is on a high level with standard deviations of about 8 cm in planimetry and 7 cm in height for the relative displacement measurements. However, the control points show standard deviations that are roughly worse by a factor 2. This can be mostly attributed to unresolved systematic errors in the photogrammetric stereo models which reduce the absolute measuring accuracy. Furthermore, the r.m.s. displacements after the strip adjustment in Table 4 match excellently the estimated accuracy showing the appropriate correction of the laser points with the adjusted strip parameters. Interestingly, the estimated accuracy is worse than the precision delivered by the new measurement technique (see Figure 7). This disagreement can be explained on the one hand by a non-perfect tie element configuration causing a weak adjustment result. On the other hand, non-linear strip deformations caused by e.g. non-adequate IMU measurements during jerky platform movements or uncalibrated non-linear scan angle errors might not sufficiently be modelled by the mathematical model (Equation 1). Moreover, another reason might be that in some cases the roof structures are not correctly represented by the intersecting planes. Similar effects could be observed by Vosselman and Maas (2001) and Maas (2002) who report on a precision of the applied TIN least-squares matching of 10 cm and estimated standard deviations after the strip adjustment (Block Eelde) of 25 cm in planimetry and 8.5 cm in height.

The measured offsets are incorporated in a strip adjustment approach to resolve for remaining shifts and rotations between LiDAR strips. Vertical shifts of a few centimeters and horizontal shifts with a magnitude higher are resolvable for the already pre-adjusted LiDAR strips. Filin and Vosselman (2004) have detected comparable horizontal offsets by analysing 10 parallel and 10 crossing strips. The resolved rotations are marginal with respect to the derived shifts, leading to the assumption discovered by Vosselman (2008) that "a simple translation of strips could already significantly improve the planimetric accuracy of the point clouds".

Furthermore, by correcting the strips with the adjusted strip parameters it is evident that horizontal discrepancies between the LiDAR strips are significantly improved by 70%. Nearly no improvement is achieved for the vertical discrepancies which are below 10 cm anyway before the adjustment. The results are comparable to the findings from Vosselman and Maas (2001), in which the degree of improvement was around 40% for the horizontal discrepancies.

6. CONCLUSIONS

Systematic residual errors, which are recognized by means of discrepancies in common areas of neighbouring LiDAR strips, are one of the main sources affecting the quality of LiDAR products. The experiments based on 8 adjacent and already pre-adjusted LiDAR strips from a test site in Southern Bavaria have pointed out that significant discrepancies still exist between individual strips. These offsets can be detected by visual inspections, a common but elaborate procedure often performed by end-users like survey administrations. With a new 3D measurement technique based on reconstructed roof shapes and roof ridge lines, remaining horizontal and vertical discrepancies between LiDAR strips now can be precisely detected with an accuracy of about 8 cm for planimetry and 7 cm for the height, thus serving as a helpful tool for a comprehensive quality control. In addition, the measurements can be incorporated as observations in a subsequent strip adjustment to resolve systematic residual errors. After the application of the corrections to each strip separately, the efficiency can be controlled using again the proposed 3D measurement technique. Note that the used dataset was already adjusted by the data provider.

Nevertheless, there are several options for future work. The measurement methods could be optimized by more automation. Investigations should also focus on an optimal configuration of tie elements. In addition, other measurement methods are worth to be evaluated for application (e.g. using straight lines or planes as control or tie elements).

REFERENCES

Ahokas, E., H. Kaartinen, and J. Hyyppä, 2004. A quality assessment of repeated airborne laser scanner observations. *Int. Arch. Photogramm. Remote Sens. Spat. Inf. Sci.*, 35 (B3), pp. 237-242.

Burman, H., 2002. Laser strip adjustment for data calibration and verification. *Int. Arch. Photogramm. Remote Sens.*, 34 (part 3A), pp. 67-72.

Filin, S., 2003. Analysis and implementation of a laser strip adjustment model. *Int. Arch. Photogramm. Remote Sens. Spat. Inf. Sci.*, 34 (3/W13), pp. 65-70.

Filin, S., and G. Vosselman, 2004. Adjustment of airborne laser altimetry strips. *Int. Arch. Photogramm. Remote Sens. Spat. Inf. Sci.*, 35 (B3), pp. 285-289.

Friess, P., 2006. Towards a rigorous methodology for airborne laser mapping. Proc. Int. Calibration and Orientation Workshop (EuroCOW 2006), Castelldefels, Spain, 25-27 Jan 2006, 7p.

Habib, A.F., A.P. Kersting, Z. Ruifang, M. Al-Durgham, C. Kim, and D.C. Lee, 2008. LiDAR strip adjustment using conjugate linear features in overlapping strips. *Int. Arch. Photogramm. Remote Sens. Spat. Inf. Sci.*, 37 (part B1), pp. 385-390.

Kager, H., 2004. Discrepancies between overlapping laser scanner strips – simultaneous fitting of aerial laser scanner strips. *Int. Arch. Photogramm. Remote Sens. Spat. Inf. Sci.*, 35 (B1), pp. 555-560.

Kilian, J., N. Haala, and M. Englich, 1996. Capture and evaluation of airborne laser scanner data. *Int. Arch. Photogramm. Remote Sens.*, 31 (B3), pp. 383-388.

Maas, H.-G., 2002. Methods for measuring height and planimetry discrepancies in airborne laserscanner data. *Photogramm. Eng. Rem. S.* 68(9), pp. 933-940.

Pfeifer, N., S. Oude Elberink, and S. Filin, 2005. Automatic tie elements detection for laser scanner strip adjustment. *Int. Arch. Photogramm. Remote Sens. Spat. Inf. Sci.*, 36 (3/W19), pp. 174-179.

Pothou, A., C. Toth, S. Karamitsos, and A. Georgopoulos, 2008. An approach to optimize reference ground control requirements for estimating LiDAR/IMU boresight misalignment. *Int. Arch. Photogramm. Remote Sens. and Spat. Inf. Sci.*, 37 (part B1), pp. 301-307.

Reitberger, J., P. Krzystek, and U. Stilla, 2008. Analysis of full waveform LiDAR data for the classification of deciduous and coniferous trees. *Int. J. Remote Sens.* 29(5), pp. 1407-1431.

Rentsch, M., and P. Krzystek, 2009. Precise quality control of LiDAR strips. Proceedings ASPRS 2009 Annual Conference, 9-13 Mar 2009, Baltimore, MD, 11 p.

Schenk, T., 2001. Modeling and analyzing systematic errors in airborne laser scanners. Technical Notes in Photogrammetry No. 19, Dept. of Civil and Environmental Eng. and Geodetic Science, The Ohio State University, Columbus, OH, 42 p.

Schenk, T., B. Csatho, and D.C. Lee, 1999. Quality control issues of airborne laser ranging data and accuracy study in an urban area. *Int. Arch. Photogramm. Remote Sens.*, 32 (3/W14), pp. 101-108.

Vosselman, G., 2008. Analysis of planimetric accuracy of airborne laser scanning surveys. *Int. Arch. Photogramm. Remote Sens. Spat. Inf. Sci.*, 37 (part B3a), pp. 99-104.

Vosselman, G., and H.-G. Maas, 2001. Adjustment and filtering of raw laser altimetry data, Proceedings OEEPE Workshop on Airborne Laserscanning and Interferometric SAR for Detailed Digital Elevation Models, Stockholm, Sweden, 01-03 March, OEEPE Publication No. 40, 62-72.